



This is a repository copy of *Preparation and characterization of quinoxaline-pyrene-based conjugated copolymers for organic photovoltaic devices*.

White Rose Research Online URL for this paper:
<http://eprints.whiterose.ac.uk/168803/>

Version: Published Version

Article:

Alqurashy, B.A., Altayeb, B.M., Alfaifi, S.Y. et al. (3 more authors) (2020) Preparation and characterization of quinoxaline-pyrene-based conjugated copolymers for organic photovoltaic devices. *Coatings*, 10 (11). 1098. ISSN 2079-6412

<https://doi.org/10.3390/coatings10111098>

Reuse

This article is distributed under the terms of the Creative Commons Attribution (CC BY) licence. This licence allows you to distribute, remix, tweak, and build upon the work, even commercially, as long as you credit the authors for the original work. More information and the full terms of the licence here:
<https://creativecommons.org/licenses/>

Takedown




If you consider content in White Rose Research Online to be in breach of UK law, please notify us by emailing eprints@whiterose.ac.uk including the URL of the record and the reason for the withdrawal request.



eprints@whiterose.ac.uk
<https://eprints.whiterose.ac.uk/>

Article

Preparation and Characterization of Quinoxaline-Pyrene-Based Conjugated Copolymers for Organic Photovoltaic Devices

Bakhet A. Alqurashy ^{1,*} , Bader M. Altayeb ², Sulaiman Y. Alfaifi ³, Majed Alawad ⁴, Ahmed Iraqi ⁵  and Imran Ali ^{2,6} 

¹ Department of Basic Science and Technologies, Community Faculty, Taibah University, Al-Madina Al-Mounawara 2898, Saudi Arabia

² Department of Chemistry, Faculty of Science, Taibah University, Al-Madina Al-Mounawara 30002, Saudi Arabia; Btayeb@taibahu.edu.sa (B.M.A.); drimran.chiral@gmail.com (I.A.)

³ Chemistry Department, Faculty of Science, King Abdulaziz University, Jeddah 80200, Saudi Arabia; salfaifi@kau.edu.sa

⁴ Material Science Research Institute, King Abdulaziz City for Science and Technology, Riyadh 12345, Saudi Arabia; moalawad@kacst.edu.sa

⁵ Department of Chemistry, University of Sheffield, Sheffield S3 7HF, UK; a.iraqi@sheffield.ac.uk

⁶ Department of Chemistry, Jamia Millia Islamia (A Central University), New Delhi 110025, India

* Correspondence: Bqourasy@taibahu.edu.sa

Received: 22 October 2020; Accepted: 12 November 2020; Published: 16 November 2020



Abstract: In this study, two novel conjugated polymers, poly(4,5,9,10-tetrakis((2-ethylhexyl)oxy)pyrene-alt-2,3-bis(3-(octyloxy)phenyl)-5,8-di(2-thienyl)-6,7-difluoroquinoxaline) (PPyQxff) and poly(4,5,9,10-tetrakis((2-ethylhexyl)oxy)pyren-alt-2,3-bis(3-(octyloxy)phenyl)-5,8-di(2-thienyl)quinoxaline) (PPyQx), consisting of quinoxaline units with and without fluorine substituents, as electron-accepting moieties and pyrene flanked with dithienyl units as electron-donating moieties were prepared via Stille polymerization reactions for use as electron donor materials in bulk heterojunction (BHJ) solar cells. PPyQxff and PPyQx were characterized by X-ray powder diffraction (XRD), gel permeation chromatography (GPC), thermogravimetric analysis (TGA), cyclic voltammetry (CV), UV–VIS absorption, and nuclear magnetic resonance (NMR) spectroscopy. PPyQxff and PPyQx revealed excellent solution processability in common organic solvents. PPyQxff and PPyQx presented decomposition temperatures above 300 °C. The inclusion of F atoms to the quinoxaline moiety made a slight reduction in the highest occupied molecular orbital (HOMO) level, relative to the unfluorinated polymer, but had no impact on the lowest unoccupied molecular orbital (LUMO) level. PPyQxff and PPyQx exhibited similar physical properties with strong and broad absorbance from 400 to 700 nm and an optical band-gap energy of 1.77 eV. The X-ray powder diffraction study indicated that PPyQxff possessed a reduced π - π stacking distance relative to PPyQx.

Keywords: pyrene; quinoxaline; conjugated polymers; donor-acceptor; organic photovoltaics

1. Introduction

High request for renewable energy sources to replace fossil fuels has prompted industrial interests and academics attention towards exploring solar energy as an alternative [1]. Commercially available photovoltaic technologies are currently dominated by inorganic solar cell technology. These are based on materials including wafer-sized, single junction crystalline silicon. They show relatively high-power conversion efficiency (PCE) (at roughly 25%) [2]. Environmental issues, manufacturing costs, and performance problems in low light level conditions do, however, present some key

drawbacks to this technology [1]. Organic photovoltaic (OPV) cells have hence become the focus of research. Organic semiconductors are able to provide improved performance as compared to their inorganic counterparts. Low-cost production processes, the ease of producing large active panels, high absorption coefficients, ease of fabrication, and light weight constitute key merits in the use of organic semiconductors in this area. OPV devices displayed lower efficiencies relative to inorganic devices; however, remarkable development of organic semiconductors has been made to boost the PCE and stability of OPV devices to make them a sustainable technology [3–5]. Up to date, Liu et al., reported the highest PCE for organic solar cells (18.22%) [6].

BHJ solar cells based on alternating donor–acceptor (D–A) conjugate polymers provide the most effective materials for use in polymer solar cells (PSCs) [7–9]. The alternation of D and A moieties on polymer backbones was found to be an efficient technique in manufacturing polymers with high-performance for BHJ applications. This observation is referred to the intramolecular charge transfer (ICT) amongst electron-deficient and electron-donor units within the copolymer segment, which allows adjusting of frontier molecular orbital energies, light absorption strength, and band gaps [10–13]. Lately, numerous numbers of D–A-conjugated copolymers have been manufactured and developed for photovoltaic devices applications. For instance, Li et al., developed a set of D–A copolymers based on quinoxaline and thiophene for use in photovoltaic devices. PDFQx-3T exhibited an optical band gap of 1.73 eV and efficiency as high as about 8% [14].

Quinoxaline moieties are widely employed in both OPVs and organic light emitting diode (OLEDs) as electron-accepting units [15–18]. In recent studies, semiconductor polymers based on quinoxaline units have been shown to exhibit remarkable PCEs, exceeding 11% [19]. This can be reflected in their ability to achieve the efficiency boundary of commercial applications of polymer photovoltaic devices. In a reported study conducted by Chen et al., fabricated organic photovoltaic cells using a copolymer of a fluorinated quinoxaline and BDT as the donor segment in (BHJ) arrangement has resulted in PSCs with a PCE of more than 8% [19,20]. More recently, the insertion of F substituents as the smallest electron-deficient groups to accepting units has attracted much attention, due to its effect on reducing unwanted steric interactions and enhancing the coplanarity of polymer chains [21,22]. Furthermore, fluorine substituents also improve the stability of the HOMO and LUMO energy levels because of its robust electron-affinity nature. Moreover, it leads to a better molecular order via noncovalent interactions, which promote planarization of the backbone of conjugated polymers. This results in favorably lowering of the band gap [20,22].

Among various building blocks with electron donating properties, pyrene has recently been targeted as an electron donor segment in copolymers for OPV applications [23,24]. Because of its moderate electron donating characteristic, pyrene-based copolymers should display a low HOMO level, which is advantageous in order to afford devices with high open circuit voltages (V_{OC}) in PCSs. Furthermore, pyrene should afford resultant polymers with efficient charge transporting properties due to its rigid and planar nature. The functionalization of the pyrene moiety at its 4-, 5-, 9-, and 10-positions displays an efficient technique to adjust the optical and electrochemical properties of the resultant polymers as well as to enable enhanced solubility [25–29]. Xu et al., stated the development of a set of acceptor-donor-acceptor organic small molecules based on pyrene. Moreover, 4.19% PCE was achieved for Pyr(EH-DPP)₂ as stated by the researchers [30].

The objective of the present study is to prepare novel donor–acceptor alternating polymers with broad absorption and narrow band gaps for BHJ solar cell applications. For the first time, pyrene as the donor (2,7-Bis(5-(trimethylstannyl)thiophen-2-yl)-4,5,9,10-tetrakis(2-ethylhexyloxy)-pyrene (M1)) was combined with fluorinated quinoxaline (2,3-Bis(3-(octyloxy)phenyl)-6,7-difluoro-5,8-bis(5-bromo-2-thienyl)quinoxaline (M2)) and with nonfluorinated quinoxaline (2,3-Bis(3-(octyloxy)phenyl)-5,8-bis(5-bromo-2-thienyl)quinoxaline (M3)) as the acceptors, where the two fluorine atoms on the quinoxaline moiety are substituted by two hydrogen atoms. A comparison of nonfluorinated and fluorinated quinoxaline-containing polymers was used to study the impact of fluorination on molecular and film structures, absorption wavelength, and HOMO and LUMO energy levels. PPyQx_{ff} and

PPyQx exhibited broad absorption bands within the wavelength range 400–700 nm with narrow optical band gaps of 1.77 eV. The polymer with the fluorine atoms (PPyQxff) had a lower molar mass and a decreased HOMO energy level.

2. Materials and Methods

All reagents and chemicals used in preparing the polymers were obtained from commercial suppliers. The materials were used as originally received, unless otherwise stated. For more information in regard to instrument and measurements see References [31,32].

2.1. Preparation of PPyQxff

PPyQxff was prepared by coupling 0.116 g (0.096 mmol) of M1 with 0.086 g (0.096 mmol) of M2. The two monomers were dissolved in 5 mL of anhydrous toluene and then, 2.00 mg (11 μ mol) of palladium (II) acetate and 7.00 mg (23 μ mol) of tri(*o*-tolyl)phosphine were added. The reaction mixture was degassed, the polymerization was undertaken under the protection of argon atmosphere, and the temperature was raised to 100 °C and left to reflux for 72 h. Then, the solution was cooled down to room temperature and concentrated and precipitated in CH₃OH. The produced precipitant was collected through filtration and subjected to Soxhlet-extraction, in turn, with CH₃OH, acetone, hexane, and CHCl₃. The CHCl₃ fraction was concentrated, and the polymer was precipitated in methanol and filtered to produce the target polymer as a purple solid (150 mg, 0.090 mmol, 55.8%). GPC results: the number-average molecular weights (M_n) = 9.8 KDa; the weight-average molecular weights (M_w) = 18.4 KDa; polydispersity index (PDI) = 1.88 and ¹H-NMR (δ_H /ppm, C₂D₂Cl₄, 100 °C, 500 MHz): 2.12–0.90 (br, 90H), 3.86 (t, 4H), 4.34 (d, 8H), 7.01 (br.d, 2H), 7.53–7.17 (br, 10H), 7.61 (br.d, 2H), 8.11 (br.d, 2H), 8.74 (br.s, 4H).

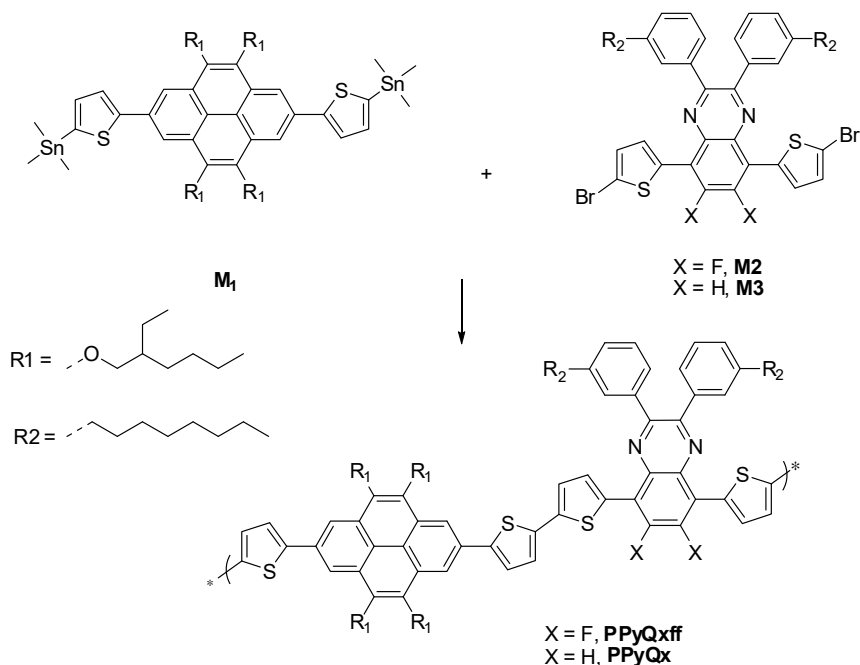
2.2. Preparation of PPyQx

PPyQx was prepared in the same method as PPyQxff, using 0.122 g (0.101 mmol) of M1, 0.087 g (0.101 mmol) of M3, 2.00 mg (11 μ mol) of palladium (II) acetate, and 7.00 mg (23 μ mol) of tri(*o*-tolyl)phosphine in 5 mL of toluene. The polymer was extracted in chloroform as a purple solid (136 mg, 0.097 mmol, 69.38%). GPC results: M_n = 10.8 KDa; M_w = 19.5 KDa; PDI = 1.80 and ¹H-NMR (δ_H /ppm, C₂D₂Cl₄, 100 °C, 500 MHz): 2.15–0.77 (br, 90H), 3.98 (t, 4H), 4.34 (d, 8H), 7.01 (br.d, 2H), 7.54–7.14 (br, 10H), 7.60 (br.d, 2H), 7.94 (br.d, 2H), 8.19 (br.d, 2H), 8.74 (br.s, 4H).

3. Results

The preparation of M1, M2, and M3 was performed according to literature procedures [24,31–34]. As shown in Scheme 1, PPyQxff and PPyQx were developed via Stille coupling polymerizations in moderate yields using a palladium (II) acetate/tri(*o*-tolyl) phosphine catalytic system. PPyQxff and PPyQx were purified through extraction with 300 mL of methanol, acetone, and hexane in order to get rid of small molecules such as monomers and oligomers and with chloroform to extract the final polymers. GPC was applied to value the number-average/weight-average molecular weights of PPyQxff and PPyQx using 1,2,4-trichlorobenzene at 140 °C as the eluent. The GPC of PPyQxff and PPyQx found to be 98/184 and 108/195 KDa with polydispersity index of 1.88 and 1.80, respectively. The slightly lower molar mass of PPyQxff in comparison to that of PPyQx is possibly as a result of the introduction of the two F substituents on the quinoxaline moieties, which leads to stronger π – π stacking and aggregation of polymer chains in solution, causing the polymer to crash out of solvent early due to fluorine sulfur interactions on neighboring polymer chains, limiting the final molar mass of the polymer. The thermal stabilities of PPyQxff and PPyQx were examined using thermogravimetric analysis (TGA) under an inert N₂ gas atmosphere at a heating scan rate of 10 °C per minute. As depicted in Figure 1. The thermal decomposition temperatures (95% weight residue) of PPyQxff and PPyQx were measured to be 333 and 335 °C, respectively, representing good thermal stabilities of both polymers. Both PPyQxff and PPyQx showed two decomposition phases. The first

one occurred at a lower temperature of 334 °C, which can be ascribed to the cleavage of the octyl chains attached to the quinoxaline acceptor moieties. The second decomposition occurred at a temperature of 441 °C, which corresponded to the loss of the rest of the attached substituents. PPyQxff and PPyQx degraded until about 52% of their molar mass was remained, and then, the curves stayed constant.



Scheme 1. Synthetic route of PPyQxff and PPyQx.

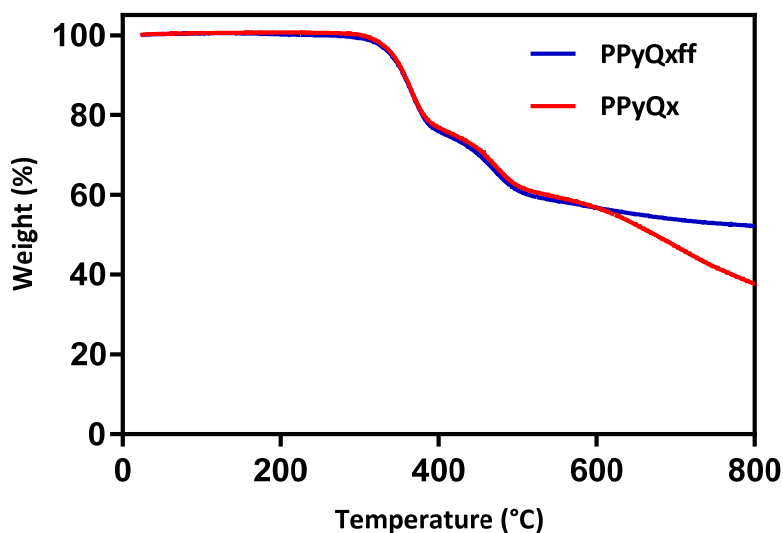


Figure 1. TGA curves of (PPyQxff) and (PPyQx).

3.1. Optical Properties

The optical properties of thin films and dilute chloroform solutions of PPyQxff and PPyQx were examined by UV–VIS absorption spectroscopy. The data are listed in Table 1. PPyQxff and PPyQx displayed similar absorption features (Figure 2). The thin films and dilute CHCl₃ solutions of the two polymers exhibit similar absorption bands between 350 and 450 nm. These absorption bands are assigned to the π – π^* transitions from the polymer backbones, while the absorption bands from 450 to 650 nm are assigned to the ICT between the quinoxaline and bis(thienyl)-pyrene units. The ICT

absorption bands of PPyQxff and PPyQx in the thin films were red shifted (by about 40 nm) with regard to those in dilute chloroform solutions, indicating a greater chain planarity polymer chains and intermolecular π - π interactions in thin films. Previous literature reports have revealed that the insertion of F atoms to donor-acceptor polymer backbones causes the absorption peaks to be blue shifted [35–37]. The inclusion of F atoms to the quinoxaline-containing polymer (PPyQxff) showed a very small blue shift (around 5 nm). We believe that the low molar mass of PPyQxff is the reason for this observation. The optical band gaps of PPyQxff and PPyQx were estimated from their absorption onsets in thin film to be at around 700 nm with a band gap of 1.77 eV. The similar optical band gaps of PPyQxff and PPyQx indicate that the addition of two F atoms in PPyQxff decreased slightly its HOMO energy level with respect to that of PPyQx but not to a significant amount.

Table 1. Characteristics of (PPyQxff) and (PPyQx).

Polymers	M_n (Da) ^a	M_w (Da) ^a	PDI	λ_{max} (nm)		$E_{g\ opt}$ (eV) ^b	HOMO (eV) ^c	LUMO (eV) ^c	$E_{g\ ele}$ (eV) ^d
				Solution	Film				
PPyQxff	9800	18,400	1.88	366, 418, 530	367, 433, 565	1.77	−5.47	−3.62	1.85
PPyQx	10,800	19,500	1.80	366, 418, 530	367, 437, 570	1.77	−5.41	−3.62	1.78

^a Measured by GPC; ^b Optical bandgap ($E_{g\ opt}$); ^c Measured by cyclic voltammetry; ^d Electrochemical band gap ($E_{g\ ele}$).

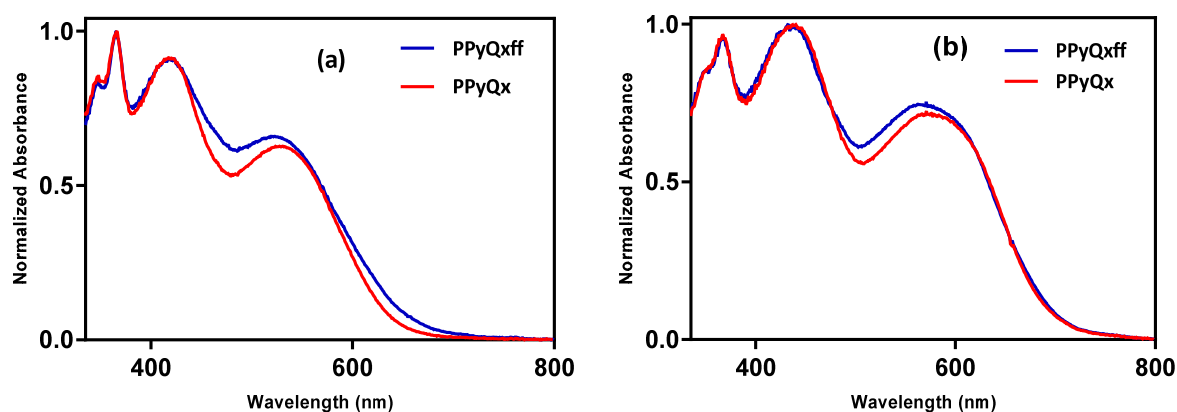


Figure 2. CHCl₃ solutions (a) and thin films (b) UV–VIS absorption spectra of PPyQxff and PPyQx.

3.2. Electrochemical Properties

The electrochemical properties of PPyQxff and PPyQx were studied by employing cyclic voltammetry (CV) analysis in order to evaluate their frontier molecular orbital energies. The CV studies were performed according to a previous published report [31]. Both HOMO and LUMO energy levels of PPyQxff and PPyQx were measured from their onset of reduction and oxidation potentials (Table 1 and Figure 3). The CV curves of PPyQxff and PPyQx reveal quasi-reversible oxidation and reduction behaviors. The HOMO energy level was calculated to be −5.47 eV for PPyQxff and −5.41 eV for PPyQx. The insertion of electron-deficient F atoms to the quinoxaline-based polymer led to a modest decrease in the HOMO energy level. Thereby, PPyQxff is expected to show slightly better air stability and a higher V_{OC} value in organic photovoltaic devices than that of the PPyQx-based devices [38,39]. The reported results agree with previous literature. The LUMO energy levels of PPyQxff and PPyQx were the same and calculated to be −3.62 eV. The wider electrochemical bandgap of PPyQxff compared to that of PPyQx is assumed to be due to the influence of the F atoms on the HOMO level of PPyQxff, hence, having a decreased HOMO and an analogous LUMO in comparison to that of PPyQx.

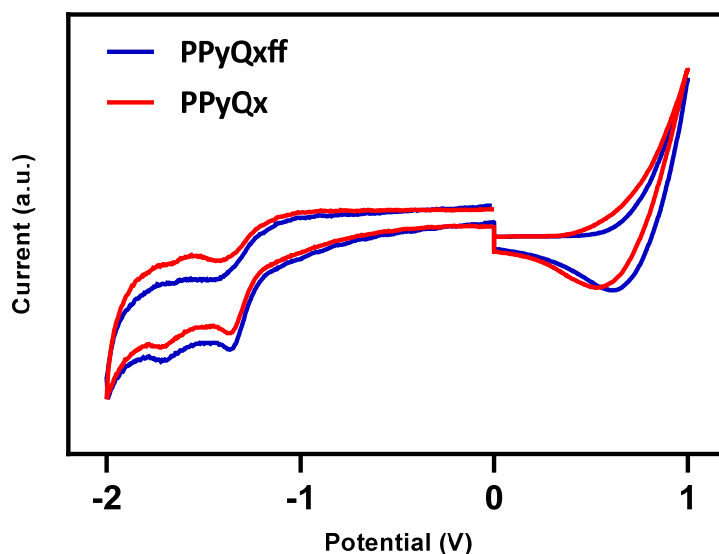


Figure 3. Cyclic voltammety curves of PPyQxff and PPyQx.

3.3. X-ray Powder Diffraction (XRD)

The crystalline properties and molecular organizations of PPyQxff and PPyQx were investigated using X-ray powder diffraction studies (XRD) (Figure 4). The XRD pattern of PPyQxff and PPyQx display poorly defined features in the small angle region at $2\theta = 3.78^\circ$, which corresponds to lamellar distances around 23.4 \AA for both polymers. PPyQxff showed an additional broad, diffuse peak in the wide-angle region at $2\theta = 23.40^\circ$, which corresponds to π - π stacking distances of 3.8 \AA . The presence of this peak for PPyQxff relative to PPyQx can be referred to the incorporation of F substituents, which could produce more intermolecular interactions between neighboring aromatic chains with F atoms. Consequently, PPyQxff should adopt a further planar structure with enhanced stacking between conjugated polymer backbones. These results clearly show that substitution of the quinoxaline repeat units with fluorine atoms leads to a better packing of polymer chains presumably through interactions between polymer chains involving fluorine substituents. Such results could have a positive effect on the charge mobility of the fluorinated polymer PPyQxff, which would have beneficial effects in its application in OPV devices.

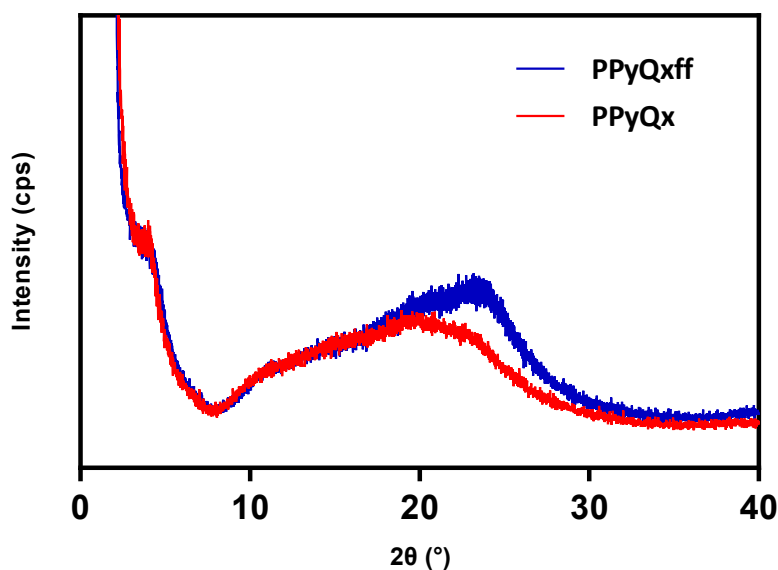


Figure 4. XRD patterns of PPyQxff and PPyQx.

4. Conclusions

In summary, two new narrow band gap donor-acceptor conjugated polymers have been prepared via the Stille coupling reaction. Both polymers were obtained in reasonable yields and the GPC data analysis indicated that polymers PPyQxff and PPyQx had weight average molecular weights ranging from 18,400 to 19,500 Da with polydispersity index of 1.88 and 1.80, respectively. The polymer with fluorine substituents on its quinoxaline repeat units PPyQxff, displayed a slightly lower molecular weight than the analogous polymer without fluorine substituents PPyQx as a consequence of its higher disposition to aggregation when compared to the nonfluorinated polymer. Both polymers displayed similar absorption maxima as well as similar band gaps (1.77 eV). Cyclic voltammetric studies indicated a slightly deeper HOMO level for the fluorinated polymer PPyQxff, nevertheless, both polymers had similar LUMO energy levels. X-ray powder diffraction studies on PPyQxff and PPyQx indicated a greater tendency of the fluorinated polymer PPyQxff towards chain aggregation with interchain stacking distances of 3.8 Å compared to 4.3 Å distances for the nonfluorinated polymer PPyQx. Further studies on the photovoltaic properties of the two polymers are currently underway.

Author Contributions: Conceptualization, B.A.A. and A.I.; validation, B.A.A. and A.I.; investigation, B.A.A., B.M.A., S.Y.A. and M.A.; resources, B.A.A., S.Y.A. and B.M.A.; writing—original draft preparation, B.A.A., B.M.A. and M.A.; writing—review and editing, A.I. and I.A.; visualization, B.A.A. and A.I.; supervision, A.I.; project administration, A.I. All authors have read and agreed to the published version of the manuscript.

Funding: This research received no external funding.

Conflicts of Interest: The authors declare no conflict of interest.

References

1. Lu, L.; Zheng, T.; Wu, Q.; Schneider, A.M.; Zhao, D.; Yu, L. Recent advances in bulk heterojunction polymer solar cells. *Chem. Rev.* **2015**, *115*, 12666–12731. [[CrossRef](#)] [[PubMed](#)]
2. Wang, E.; Wang, L.; Lan, L.; Luo, C.; Zhuang, W.; Peng, J.; Cao, Y. High-performance polymer heterojunction solar cells of a polysilfluorene derivative. *Appl. Phys. Lett.* **2008**, *92*, 2–5. [[CrossRef](#)]
3. Henson, Z.B.; Müllen, K.; Bazan, G.C. Design strategies for organic semiconductors beyond the molecular formula. *Nat. Chem.* **2012**, *4*, 699–704. [[CrossRef](#)]
4. Dennler, G.; Scharber, M.C.; Brabec, C.J. Polymer-fullerene bulk-heterojunction solar cells. *Adv. Mater.* **2009**, *21*, 1323–1338. [[CrossRef](#)]
5. Ameri, T.; Khoram, P.; Min, J.; Brabec, C.J. Organic ternary solar cells: A review. *Adv. Mater.* **2013**, *25*, 4245–4266. [[CrossRef](#)]
6. Liu, Q.; Jiang, Y.; Jin, K.; Qin, J.; Xu, J.; Li, W.; Xiong, J.; Liu, J. 18% Efficiency organic solar cells. *Sci. Bull.* **2020**, *65*, 272–275. [[CrossRef](#)]
7. Kitamura, C.; Tanaka, S.; Yamashita, Y. Design of narrow-bandgap polymers. Syntheses and properties of monomers and polymers containing aromatic-donor and o-quinoid-acceptor units. *Chem. Mater.* **1996**, *8*, 570–578. [[CrossRef](#)]
8. Price, S.C.; Stuart, A.C.; Yang, L.; Zhou, H.; You, W. Fluorine substituted conjugated polymer of medium band gap yields 7% efficiency in polymer-fullerene solar cells. *J. Am. Chem. Soc.* **2011**, *133*, 4625–4631. [[CrossRef](#)]
9. Chen, H.C.; Chen, Y.H.; Liu, C.C.; Chien, Y.C.; Chou, S.W.; Chou, P.T. Prominent short-circuit currents of fluorinated quinoxaline-based copolymer solar cells with a power conversion efficiency of 8.0%. *Chem. Mater.* **2012**, *24*, 4766–4772. [[CrossRef](#)]
10. Bronstein, H.; Frost, J.M.; Hadipour, A.; Kim, Y.; Nielsen, C.B.; Ashraf, R.S.; Rand, B.P.; Watkins, S.; McCulloch, I. Effect of fluorination on the properties of a donor-acceptor copolymer for use in photovoltaic cells and transistors. *Chem. Mater.* **2013**, *25*, 277–285. [[CrossRef](#)]
11. Duan, R.; Ye, L.; Guo, X.; Huang, Y.; Wang, P.; Zhang, S.; Zhang, J.; Huo, L.; Hou, J. Application of two-dimensional conjugated benzo[1,2-b:4,5-b']dithiophene in quinoxaline-based photovoltaic polymers. *Macromolecules* **2012**, *45*, 3032–3038. [[CrossRef](#)]

12. Chochos, C.L.; Choulis, S.A. How the structural deviations on the backbone of conjugated polymers influence their optoelectronic properties and photovoltaic performance. *Prog. Polym. Sci.* **2011**, *36*, 1326–1414. [[CrossRef](#)]
13. Wang, N.; Chen, Z.; Wei, W.; Jiang, Z. Fluorinated benzothiadiazole-based conjugated polymers for high-performance polymer solar cells without any processing additives or post-treatments. *J. Am. Chem. Soc.* **2013**, *135*, 17060–17068. [[CrossRef](#)] [[PubMed](#)]
14. Alqurashy, B.A.; Li, Y.; Ko, S.J.; Park, S.Y.; Choi, H.; Nguyen, T.L.; Uddin, M.A.; Kim, T.; Hwang, S.; Kim, J.Y.; et al. Quinoxaline–thiophene based thick photovoltaic devices with an efficiency of ~8%. *J. Mater. Chem. A* **2016**, *4*, 9967–9976. [[CrossRef](#)]
15. Günes, S.; Neugebauer, H.; Sariciftci, N.S. Conjugated polymer-based organic solar cells. *Chem. Rev.* **2007**, *107*, 1324–1338. [[CrossRef](#)] [[PubMed](#)]
16. Reddy, M.R.; Han, S.H.; Lee, J.Y.; Seo, S.Y. Synthesis and characterization of quinoxaline derivative for high performance phosphorescent organic light-emitting diodes. *Dye. Pigment.* **2018**, *153*, 132–136. [[CrossRef](#)]
17. Chang, D.W.; Lee, H.J.; Kim, J.H.; Park, S.Y. Novel quinoxaline-based organic sensitizers for dye-sensitized solar cells. *Org. Lett.* **2011**, *13*, 3880–3883. [[CrossRef](#)]
18. Wang, E.; Hou, L.; Wang, Z.; Hellström, S.; Zhang, F.; Inganäs, O.; Andersson, M.R. An easily synthesized blue polymer for high-performance polymer solar cells. *Adv. Mater.* **2010**, *22*, 5240–5244. [[CrossRef](#)]
19. Liu, M.; Gao, Y.; Zhang, Y.; Liu, Z.; Zhao, L. Quinoxaline-based conjugated polymers for polymer solar cells. *Polym. Chem.* **2017**, *8*, 4613–4636. [[CrossRef](#)]
20. Dang, D.; Chen, W.; Yang, R.; Zhu, W.; Mammo, W.; Wang, E. Fluorine substitution enhanced photovoltaic performance of a D-A 1-D-A2 copolymer. *Chem. Commun.* **2013**, *49*, 9335–9337. [[CrossRef](#)]
21. Liu, D.; Zhao, W.; Zhang, S.; Ye, L.; Zheng, Z.; Cui, Y.; Chen, Y.; Hou, J. Highly efficient photovoltaic polymers based on benzodithiophene and quinoxaline with deeper HOMO levels. *Macromolecules* **2015**, *48*, 5172–5178. [[CrossRef](#)]
22. Zhao, B.; Wu, H.; Liu, S.; Luo, G.; Wang, W.; Guo, Z.; Wei, W.; Gao, C.; An, Z. Efficient alternating polymer based on benzodithiophene and di-fluorinated quinoxaline derivatives for bulk heterojunction photovoltaic cells. *Polymer (Guildf)*. **2017**, *116*, 35–42. [[CrossRef](#)]
23. Wang, N.; Bao, X.; Yan, Y.; Ouyang, D.; Sun, M.; Roy, V.A.L.; Lee, C.S.; Yang, R. Synthesis and photovoltaic properties of conjugated D-A copolymers based on thienyl substituted pyrene and diketopyrrolopyrrole for polymer solar cells. *J. Polym. Sci. Part A Polym. Chem.* **2014**, *52*, 3198–3204. [[CrossRef](#)]
24. Alqurashy, B.A. Preparation and physical characterization of pyrene and pyrrolo[3,4-c]pyrrole-1,4-dione-based copolymers. *ChemistryOpen* **2019**, *8*, 429–433. [[CrossRef](#)]
25. Merz, J.; Dietz, M.; Vonhausen, Y.; Wöber, F.; Friedrich, A.; Sieh, D.; Krummenacher, I.; Braunschweig, H.; Moos, M.; Holzapfel, M.; et al. Synthesis, photophysical and electronic properties of new red-to-NIR emitting donor–Acceptor pyrene derivatives. *Chem. Eur. J.* **2020**, *26*, 438–453. [[CrossRef](#)]
26. Figueira-Duarte, T.M.; Müllen, K. Pyrene-based materials for organic electronics. *Chem. Rev.* **2011**, *111*, 7260–7314. [[CrossRef](#)]
27. Zöphel, L.; Beckmann, D.; Enkelmann, V.; Chercka, D.; Rieger, R.; Müllen, K. Asymmetric pyrene derivatives for organic field-effect transistors. *Chem. Commun.* **2011**, *47*, 6960–6962. [[CrossRef](#)]
28. Cai, G.; Xue, P.; Chen, Z.; Li, T.; Liu, K.; Ma, W.; Lian, J.; Zeng, P.; Wang, Y.; Han, R.P.S.; et al. High-performance mid-bandgap fused-pyrene electron acceptor. *Chem. Mater.* **2019**, *31*, 6484–6490. [[CrossRef](#)]
29. Liu, S.Y.; Liu, W.Q.; Xu, J.Q.; Fan, C.C.; Fu, W.F.; Ling, J.; Wu, J.Y.; Shi, M.M.; Jen, A.K.Y.; Chen, H.Z. Pyrene and diketopyrrolopyrrole-based oligomers synthesized via direct arylation for OSC applications. *ACS Appl. Mater. Interfaces* **2014**, *6*, 6765–6775. [[CrossRef](#)]
30. Xu, J.; Liu, W.; Liu, S.; Ling, J.; Mai, J.; Lu, X.; Li, C.; Jen, A.K.; Chen, H. A-D-A small molecule donors based on pyrene and diketopyrrolopyrrole for organic solar cells. *Sci. China Chem.* **2017**, *60*, 561–569. [[CrossRef](#)]
31. Alqurashy, B.A.; Cartwright, L.; Iraqi, A.; Zhang, Y.; Lidzey, D.G. Pyrene–benzothiadiazole-based copolymers for application in photovoltaic devices. *Polym. Adv. Technol.* **2017**, *28*, 193–200. [[CrossRef](#)]
32. Alqurashy, B.A.; Iraqi, A.; Zhang, Y.; Lidzey, D.G. Preparation and photovoltaic properties of pyrene-thieno[3,4-c]pyrrole-4,6-dione-based donor-acceptor polymers. *Eur. Polym. J.* **2016**, *85*, 225–235. [[CrossRef](#)]
33. Park, S.M.; Yoon, Y.; Jeon, C.W.; Kim, H.; Ko, M.J.; Lee, D.K.; Kim, J.Y.; Son, H.J.; Kwon, S.K.; Kim, Y.H.; et al. Synthesis of phenanthro[1,10,9,8-cdefg]carbazole-based conjugated polymers for organic solar cell applications. *J. Polym. Sci. Part A Polym. Chem.* **2014**, *52*, 796–803. [[CrossRef](#)]

34. Dang, D.; Xiao, M.; Zhou, P.; Shi, J.; Tao, Q.; Tan, H.; Wang, Y.; Bao, X.; Liu, Y.; Wang, E.; et al. Manipulating backbone structure with various conjugated spacers to enhance photovoltaic performance of D-A-type two-dimensional copolymers. *Org. Electron.* **2014**, *15*, 2876–2884. [[CrossRef](#)]
35. You, J.; Dou, L.; Yoshimura, K.; Kato, T.; Ohya, K.; Moriarty, T.; Emery, K.; Chen, C.C.; Gao, J.; Li, G.; et al. A polymer tandem solar cell with 10.6% power conversion efficiency. *Nat. Commun.* **2013**, *4*, 1446. [[CrossRef](#)] [[PubMed](#)]
36. Zhang, Y.; Chien, S.C.; Chen, K.S.; Yip, H.L.; Sun, Y.; Davies, J.A.; Chen, F.C.; Jen, A.K.Y. Increased open circuit voltage in fluorinated benzothiadiazole-based alternating conjugated polymers. *Chem. Commun.* **2011**, *47*, 11026–11028. [[CrossRef](#)]
37. Kroon, R.; Gehlhaar, R.; Steckler, T.T.; Henriksson, P.; Müller, C.; Bergqvist, J.; Hadipour, A.; Heremans, P.; Andersson, M.R. New quinoxaline and pyridopyrazine-based polymers for solution-processable photovoltaics. *Sol. Energy Mater. Sol. Cells* **2012**, *105*, 280–286. [[CrossRef](#)]
38. Kim, J.; Yun, M.H.; Kim, G.H.; Lee, J.; Lee, S.M.; Ko, S.J.; Kim, Y.; Dutta, G.K.; Moon, M.; Park, S.Y.; et al. Synthesis of PCDTBT-based fluorinated polymers for high open-circuit voltage in organic photovoltaics: Towards an understanding of relationships between polymer energy levels engineering and ideal morphology control. *ACS Appl. Mater. Interfaces* **2014**, *6*, 7523–7534. [[CrossRef](#)]
39. Yang, J.; Zhao, Z.; Wang, S.; Guo, Y.; Liu, Y. Insight into high-performance conjugated polymers for organic field-effect transistors. *Chem* **2018**, *4*, 2748–2785. [[CrossRef](#)]

Publisher’s Note: MDPI stays neutral with regard to jurisdictional claims in published maps and institutional affiliations.



© 2020 by the authors. Licensee MDPI, Basel, Switzerland. This article is an open access article distributed under the terms and conditions of the Creative Commons Attribution (CC BY) license (<http://creativecommons.org/licenses/by/4.0/>).